

RESEARCH ARTICLE

Class I KNOX transcription factors promote differentiation of cambial derivatives into xylem fibers in the *Arabidopsis* hypocotyl

Daniela Liebsch^{1,§}, Widi Sunaryo^{2,*}, Mattias Holmlund¹, Mikael Norberg¹, Jing Zhang³, Hardy C. Hall¹, Hanna Helizon^{1,‡}, Xu Jin^{1,2}, Ykä Helariutta³, Ove Nilsson¹, Andrea Polle² and Urs Fischer^{1,2,¶}

ABSTRACT

The class I KNOX transcription factors SHOOT MERISTEMLESS (STM) and KNAT1 are important regulators of meristem maintenance in shoot apices, with a dual role of promoting cell proliferation and inhibiting differentiation. We examined whether they control stem cell maintenance in the cambium of *Arabidopsis* hypocotyls, a wood-forming lateral meristem, in a similar fashion as in the shoot apical meristem. Weak loss-of-function alleles of *KNAT1* and *STM* led to reduced formation of xylem fibers – highly differentiated cambial derivatives – whereas cell proliferation in the cambium was only mildly affected. In a *knat1;stm* double mutant, xylem fiber differentiation was completely abolished, but residual cambial activity was maintained. Expression of early and late markers of xylary cell differentiation was globally reduced in the *knat1;stm* double mutant. *KNAT1* and *STM* were found to act through transcriptional repression of the meristem boundary genes *BLADE-ON-PETIOLE 1 (BOP1)* and *BOP2* on xylem fiber differentiation. Together, these data indicate that, in the cambium, *KNAT1* and *STM*, contrary to their function in the shoot apical meristem, promote cell differentiation through repression of BOP genes.

KEY WORDS: *Arabidopsis*, Cambium, Class I KNOX transcription factors, Secondary growth, Stem cell maintenance

INTRODUCTION

In higher plants, the bulk of cell divisions occur in tissues with a low degree of differentiation, the so-called meristems. Meristems are either placed at the tips of plant organs, i.e. apical meristems, or subapically, as lateral meristems. Derivatives of stem cells in apical meristems elongate along the main growth axes, whereas daughter cells of lateral meristems, e.g. of the vascular cambium, expand mainly radially and therefore contribute to the increment in diameter of plant organs. As both apical and lateral meristems fulfill the same basic meristematic functions of stem cell specification, maintenance, cell proliferation and differentiation, it has been suggested that these processes are regulated by the same or paralogous genes across different types of meristems (Groover et al., 2006; Aichinger et al., 2012). Stem cell maintenance in the shoot apical meristem

(SAM) is partly directed by a negative-feedback loop between the homeodomain transcription factor WUSCHEL (*WUS*) and the peptide ligand-producing gene *CLAVATA3 (CLV3)* (Aichinger et al., 2012). *WUS* is expressed in the stem cell niche (organizing center) of the SAM from where the *WUS* protein can move to the stem cells to activate *CLV3* expression in order to control the size of the stem cell population (Yadav et al., 2011). *CLV3* peptide signaling in turn represses *WUS* transcription, resulting in negative-feedback regulation of *WUS* (Schoof et al., 2000; Brand et al., 2000). Similarly, *WUS* and *CLV3* paralogs control stem cell behavior in the root apical meristem (*WOX5* and *CLE40*) (Stahl et al., 2009) and the cambium (*WOX4* and *CLE41/44*) (Hirakawa et al., 2010), suggesting that paralogous genes regulate stem cell maintenance across different classes of meristems.

Independently of the *WUS-CLV3* regulatory circuit, the class I KNOX homeodomain transcription factor SHOOT MERISTEMLESS (*STM*) contributes to meristem maintenance in the SAM (Lenhard et al., 2002). *STM* is expressed throughout the meristem but not at the place of incipient leaves (Long and Barton, 1998). *STM*-null mutants in the *Ler* background fail to establish a SAM during late embryogenesis and weak mutant alleles lead to abortion of the SAM after the formation of only a few leaves (Endrizzi et al., 1996). *KNAT1*, another member of the class I KNOX family, is expressed in a similar pattern to *STM* (Lincoln et al., 1994) and acts redundantly with *STM* on meristem maintenance (Byrne et al., 2002). Furthermore, the *stm* meristem phenotype can be rescued by *KNAT1* overexpression (Scofield et al., 2013). Together, these data have led to the interpretation of *STM* and *KNAT1* as being required to prevent cell differentiation at the site of their expression and hence to keep cells meristematic. Conversely, absence of their transcripts from incipient leaves is thought to allow differentiation, as a consequence of which organogenesis from meristematic tissue can take place.

In wood-forming tissues, the cambium forms radial files of daughter cells that undergo rapid differentiation into xylem and phloem. In the xylem, a phase of radial cell expansion is followed by secondary cell wall (SCW) deposition, which represents a structural barrier preventing cell division and renders differentiation irreversible. In *Arabidopsis*, the establishment of the cambium in the hypocotyl is already completed early in development, approximately 2 weeks after germination (Busse and Evert, 1999). At this developmental stage, referred to as xylem I, xylary derivatives differentiate into vessel cells and chlorophyll-containing parenchymatic cells with unligified walls (Chaffey et al., 2002). Later in development, upon flowering, xylem fibers with lignified SCWs are formed instead of parenchymatic cells (a phase that is referred to as xylem II) (Chaffey et al., 2002; Sibout et al., 2008), resulting in a similar anatomy to that of angiosperm wood. In contrast to the *Arabidopsis* inflorescence, the hypocotyl contains a continuous cylindrical cambium without disturbances of traces from lateral organs. Furthermore, an apical-basal developmental gradient with internodes of different developmental stages, as is characteristic

¹Umeå Plant Science Centre, Department of Forest Genetics and Plant Physiology, Swedish University of Agricultural Sciences, Umeå SE-901 83, Sweden.

²Department of Forest Botany and Tree Physiology, University of Göttingen, Göttingen DE-37077, Germany. ³Institute of Biotechnology, University of Helsinki, Helsinki 00014, Finland.

*Present address: Department of Agroecotechnology, Faculty of Agriculture, Mulawarman University, Samarinda, Indonesia. ⁴Present address: Institute of Plant Physiology, Justus-Liebig-University Giessen, Giessen DE-35390, Germany.

[§]These authors contributed equally to this work

[¶]Author for correspondence (urs.fischer@slu.se)

for the *Arabidopsis* stem, is absent in the hypocotyl (Ragni and Hardtke, 2013; Schuetz et al., 2013).

Despite the fact that *STM* homologs are expressed in the vascular cambium of *Populus* trees (Schrader et al., 2004; Groover et al., 2006) and although it was previously noted that *STM* in *Arabidopsis* is not exclusively expressed in the SAM but also subapically in tissues related to the vasculature, little attention has been paid to its function outside the SAM (Sanchez et al., 2012; Aichinger et al., 2012). Although phenotypes outside the SAM have been reported for *knat1* mutants, e.g. downward-pointing siliques (Ragni et al., 2008), premature floral organ abscission (Shi et al., 2011) and aberrant lignification patterns in the inflorescence stem (Mele et al., 2003), the role of *KNAT1* in cambium maintenance and differentiation of cambial derivatives has not yet been investigated. We made use of weak *stm* and *knat1* mutant alleles and the simple anatomy of *Arabidopsis* hypocotyls in order to study whether their function as repressors of differentiation has been co-opted by the cambium during the evolution of secondary growth.

RESULTS

KNAT1 and *STM* are expressed in the cambial zone and in the developing xylem

Arabidopsis hypocotyls grow radially from the cambium, the derivatives of which undergo gradual differentiation either into xylem fibers, parenchyma and vessels to the inner side or into phloem to the outer side. If *STM* and *KNAT1* keep cambial cells undifferentiated and meristematic, similar to the SAM, their expression is expected to be highest in dividing cells of the cambium and absent in differentiating cambial daughter cells. In the hypocotyl, *pKNAT1::GUS* and *pSTM::GUS* activities were highest in the cambial zone, but unlike in the SAM, where *STM* and *KNAT1* transcripts are not present at positions of organogenesis, they were also expressed in the phloem and in developing and mature xylem fibers (Fig. 1A–D). *KNAT1* and *STM* transcripts were equally abundant in dissected hypocotyls of 6-week-old plants and in inflorescence meristems of the same age (Fig. 1E). Similar strength of expression in the two different types of meristems supports the hypothesis of *KNAT1* and *STM* playing a role outside of apical meristems, but presence of their transcripts in differentiating and even mature cambial derivatives indicates that these two transcription factors fulfill additional or different tasks in the cambium than in the SAM.

Mutations in *KNAT1* and *STM* cause reduced xylem fiber formation

We then isolated mutants of *STM* and *KNAT1* in order to functionally address their role in the cambium of the hypocotyl. Because in plants homozygous for strong *stm* loss-of-function alleles, the SAM aborts early or is not established (Barton and Poethig, 1993; Endrizzi et al., 1996), we identified weak loss-of-function mutants in *STM* [*stm-GK*; NASC (N409575)] and *KNAT1* (*knat1^{bp-9}*). *knat1^{bp-9}* and *stm-GK* carry a T-DNA insertion in the first and second intron, respectively, which caused a reduction of the wild-type transcript levels in both mutants by more than two orders of magnitude (supplementary material Fig. S1A). Both mutants accumulated the same amount of aerial biomass as wild type 6 weeks after germination (supplementary material Fig. S1B). Hypocotyls of *knat1^{bp-9}* and *stm-GK* mutants were smaller in diameter than wild type (supplementary material Fig. S2) and transverse sections through the hypocotyl of 6-week-old plants revealed a reduction of the ratio between xylem II and total xylem, indicative of reduced xylem fiber formation (Fig. 2A,B). Hypocotyl

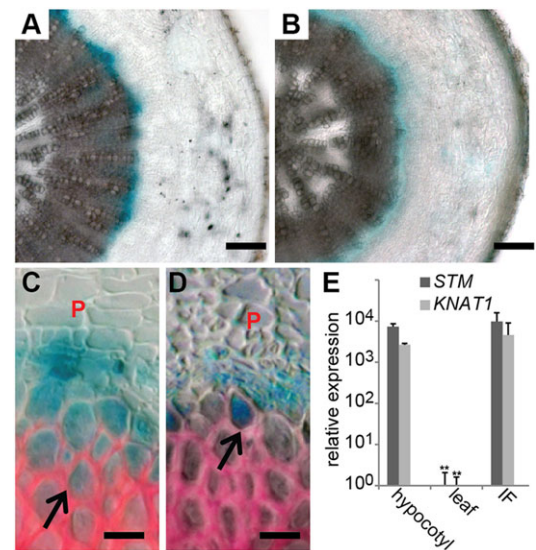


Fig. 1. *KNAT1* and *STM* are expressed in the cambial zone. (A–D) GUS reporter activity in transverse sections of 6-week-old hypocotyls. (C, D) Pictures show higher magnifications of the area around the cambial zone. Arrows indicate mature xylem fibers expressing the GUS reporter gene. P, phloem. Phloroglucinol was used as a counterstain; lignified cell walls appear in red. (A, C) *pKNAT1::GUS*. (B, D) *pSTM::GUS*. Scale bars: 200 μ m in A, B; 10 μ m in C, D. (E) qRT-PCR results. RNA was extracted from different parts of 6-week-old plants. IF, inflorescence meristems. Data are mean \pm s.d. of three independent experiments. ** $P < 0.01$, *t*-test in comparison with hypocotyl. Values are expressed relative to *ACT2* expression and normalized to expression in leaves (=1).

diameter and xylem II formation were similarly reduced in *stm-6*, another weak mutant, as in *stm-GK*, whereas in the null mutant *knat1^{bp-11}* (de la Paz et al., 2012), xylem fiber differentiation was almost entirely abolished (Fig. 2B; supplementary material Fig. S2). By contrast, single mutants for all the other members of the KNOX gene family did not display reduced xylem II (supplementary material Fig. S2). Similar to their hypocotyls, in the oldest internode of *knat1^{bp-9}* and *stm-GK* inflorescence stems we frequently observed vascular bundles that did not form fibers (supplementary material Fig. S3).

Hypocotyls of *stm-GK* and *knat1^{bp-9}* showed only small differences in total cambial activity, but instead of fibers (xylem II), they formed more xylem parenchyma cells (xylem I) per radial cambial cell file than did wild type (Fig. 2C). In contrast to xylem production, the number of phloem cells was not altered in hypocotyls of *stm-GK* and *knat1^{bp-9}*. In order to test whether diminished cell expansion contributed to reduced hypocotyl diameters of *knat1* and *stm* mutants, we measured radial cell expansion of cambial derivatives, which is an early step in their differentiation into vessels or fibers. Both fibers and vessels of *stm-GK* and *knat1^{bp-9}* did not expand to the same luminal areas as observed in mature vessels and fibers of wild-type hypocotyls (Fig. 3A). The degree of reduction of luminal area accounted for smaller diameters of mutant hypocotyls, indicating that *KNAT1* and *STM* were required for early steps of xylem cell differentiation. We then examined expression patterns of *ATHB8*, an early marker of vascularization that, when overexpressed, promotes xylem fiber and vessel differentiation (Baima et al., 1995; Gardiner et al., 2011). In wild type, *pATHB8::GUS* was expressed in the cambium and developing xylem, peaking in cell files, which give rise to xylem vessel cells, and to a lesser extent in cells at the origin of fiber cell files. By contrast, *pATHB8::GUS* expression was nearly absent in xylem fiber cell files in *stm-GK* and *knat1^{bp-9}* (Fig. 3B–D). Taken

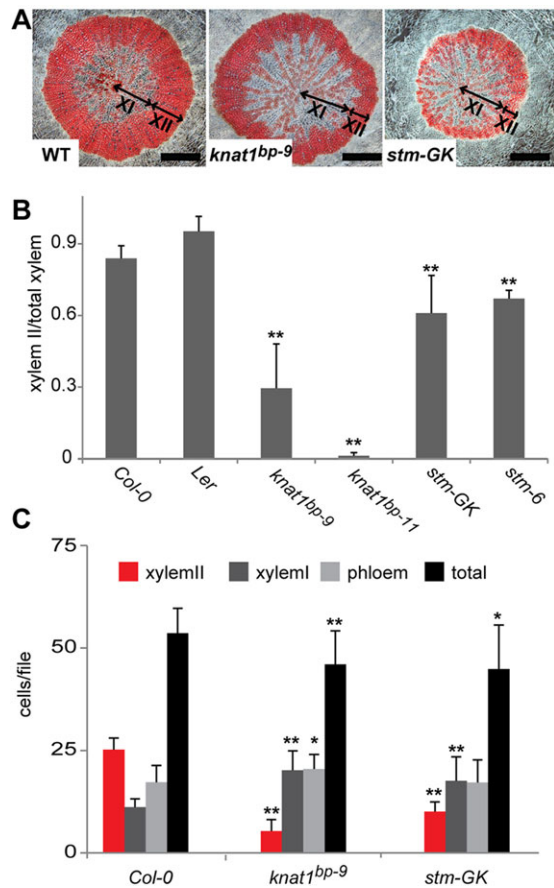


Fig. 2. *KNAT1* and *STM* are required for xylem fiber formation.

(A) Transverse sections of 6-week-old hypocotyls stained with phloroglucinol to visualize lignified cell walls (red). Scale bars: 200 μm . XI, xylem I; XII, xylem II. (B) Ratio between the area occupied by xylem II and total xylem area in transverse sections from 6-week-old hypocotyls. Data are mean \pm s.d. of three independent experiments per genotype, with each three hypocotyls per experiment. *stm-6* in *Ler-0* background. (C) Cambial cell divisions. Data represent the average number of cambial daughter cells per cambial cell file (mean \pm s.d. of three individual hypocotyls per genotype). For each hypocotyl, four cell files from transverse sections of 6-week-old hypocotyls were scored. (B,C) *t*-test; * $P < 0.05$; ** $P < 0.01$; comparing mutants with wild type.

together, reduction of *STM* and *KNAT1* expression impaired early events of differentiation of cambial daughter cells into xylem fibers, whereas it only weakly affected overall cambial cell division activity. Promotion of xylem fiber differentiation by *STM* and *KNAT1* stands in sharp contrast to their proposed function of preventing differentiation of meristematic cells in the SAM.

Final radial diameter of cambial derivatives is a result of the cell expansion rate and the residence time in the expansion zone (Skene, 1969; Cuny et al., 2014). Hence, large expansion zones, as observed for example during early wood formation, correlate with big luminal areas, whereas short expansion zones are associated with smaller lumina of cambial derivatives. Smaller cells in *stm* and *knat1* mutants could therefore be a consequence of reduced residence time of cambial derivatives in the expansion zone rather than defective rate of cell expansion. We measured the radial dimension of the expansion zone, including the cambium, with the help of the JIM13 cell wall epitope (Hall et al., 2013), which marks mature phloem bundles and SCW of xylem fibers and vessels (supplementary material Fig. S4). At the time of transition to flowering, the cambium-expansion zones of *knat1^{bp-9}* and *stm-GK* hypocotyls

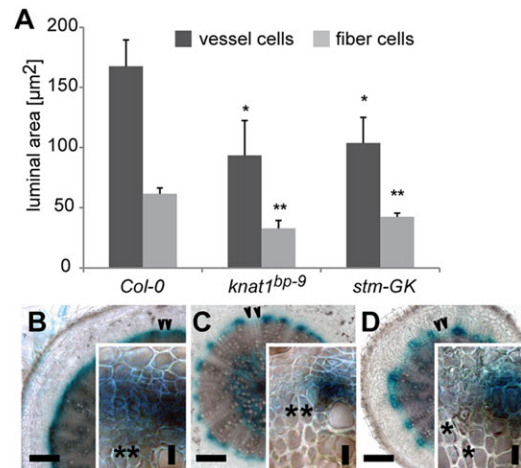


Fig. 3. *KNAT1* and *STM* control early events in vascular differentiation.

(A) Cell expansion of xylem fibers and vessels. Data represent averages of transverse luminal area \pm s.d. calculated from three different independent experiments. Thirty cells per genotype and experiment were measured from transverse sections of 6-week-old hypocotyls. *t*-test; * $P < 0.05$; ** $P < 0.01$; comparing mutants with wild type. (B–D) GUS reporter activity for *pAtHB8::GUS* in transverse sections of 6-week-old hypocotyls: (B) *pAtHB8::GUS*; (C) *knat1^{bp-9}::pAtHB8::GUS*; and (D) *stm-GK::pAtHB8::GUS*. Arrowheads, xylem fiber cell files; asterisks, mature fiber cells. Scale bars: 200 μm ; 20 μm in insets.

were of similar size to those in wild type. One week after transition to flowering, when the first mature xylem fibers had been formed, the cambium-expansion zone was reduced to about one-third of its previous size in wild type. By contrast, in both mutants, the cambium-expansion zones were significantly larger 1 week after transition to flowering than they were in wild type. Thus, the cell expansion defect observed in the mutants cannot be explained by a reduction in expansion zone sizes, suggesting that *STM* and *KNAT1* have a direct positive impact on the rate of cell expansion.

***KNAT1* function on fiber formation is local and independent of flowering time regulation**

Even though expression patterns support a local function of *KNAT1* and *STM* in the hypocotyl, effects on fiber differentiation could be indirect, e.g. mediated through a mobile hormone-like factor derived from the SAM. Class I KNOX genes have previously been suggested to regulate the biosynthesis of the plant hormones cytokinin and GA in the SAM (Jasinski et al., 2005). Furthermore, graft-transmissible GA promotes fiber formation in the hypocotyl (Ragni et al., 2011). To address the issue of whether class I KNOX genes act locally in the hypocotyl/root to influence fiber differentiation, we used reciprocal grafting experiments. As we could not recover viable plants from graftings involving *stm*, we focused on reciprocal graftings with *knat1*. Five-day-old wild-type (*Ler*) hypocotyls were grafted on *knat1^{bp-1}* stocks and hypocotyls of 6-week-old plants were sampled. The hypocotyl scion above the grafting junction was white (normal for the wild type), whereas the mutant stock was dark green (typical for *knat1* hypocotyls) (supplementary material Fig. S5). Transverse sections of the grafted stocks, 3 mm below the grafting junction, were analyzed (Fig. 4). No phenotypic alterations were observed in wild-type hypocotyls carrying *knat1^{bp-1}* scions, whereas in *knat1^{bp-1}* hypocotyls carrying a wild-type shoot, fiber formation was affected to a similar degree than in graftings between *knat1^{bp-1}* stocks and scions. Reduced xylem fiber formation indicated that wild-type shoots were not sufficient to rescue the fiber differentiation phenotype in *knat1^{bp-1}*

hypocotyls. As expression of the typical *knat1* phenotype in the hypocotyl did not depend on the presence of defective *KNAT1* in the shoot/scion, *KNAT1* probably acts locally, in the hypocotyl or root, on xylem fiber differentiation.

In wild type, transition to xylem II development took place after the formation of ~11 parenchymatic cells per cambial cell file (Fig. 2C). By contrast, onset of the xylem II phase was delayed in *knat1^{bp-9}* (after 19 cells) and *stm-GK* (after 15 cells). Initiation of SCW deposition in xylem fibers of the hypocotyl correlates with induction of flowering; in recombinant inbred lines of a Uk-1×Sav-0 cross, the major QTL for fiber differentiation localizes to *FLC*, a negative regulator of flowering time (Sibout et al., 2008). We therefore tested whether delayed flowering accounts for delayed xylem II development in *stm* and *knat1* mutants. Although weak *stm* mutants rarely form flowers (Endrizzi et al., 1996; Felix et al., 1996), both *knat1* and wild type flowered after the formation of ~11 rosette and three cauline leaves, and also bolted at the same time (Fig. 5). Reduced xylem fiber formation in *knat1* was therefore not a consequence of delayed flowering, and *KNAT1* seems to act downstream of or in parallel to regulators of flowering time. Notably, both mutants produced the first xylem fibers 1-2 weeks later than the wild type, where the first mature fibers were observed 4 weeks after germination, shortly after initiation of flowering took place (supplementary material Fig. S6). In wild-type hypocotyls,

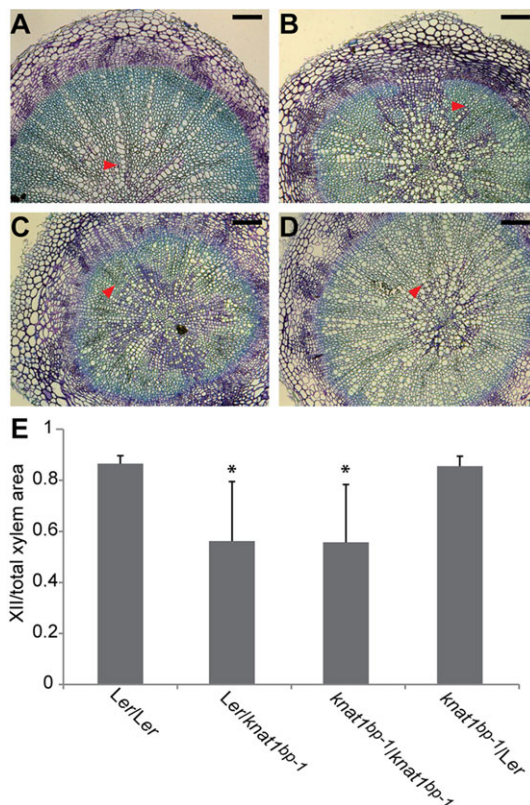


Fig. 4. *KNAT1* acts locally on xylem fiber formation. (A–D) Toluidine Blue stained transverse sections of grafted stocks, 3 mm below grafting junction. Scale bars: 100 μ m. (A) *Ler* scion/*Ler* stock (*Ler/Ler*); (B) *Ler/knat1^{bp-1}*; (C) *knat1^{bp-1}/knat1^{bp-1}*; (D) *knat1^{bp-1}/Ler*. Arrowheads indicate the boundary between xylem I and xylem II. (E) Data are mean \pm s.d. of area occupied by xylem II in relation to total xylem area. $n=4$ for all combinations except for *Ler/knat1^{bp-1}* ($n=8$). *t*-test; * $P<0.05$. Xylem II/xylem ratio was significantly lower in stocks of *Ler/knat1^{bp-1}* when compared with *Ler/Ler* ($P<0.05$). No differences in xylem II formation were observed between stocks of *knat1^{bp-1}/Ler* and *Ler/Ler* ($P>0.05$).

xylem fiber production stopped between 6 and 7 weeks after germination, corresponding to the time point when the first silique was completely senescent. Similarly, fiber production ceased after 6 and 7 weeks in *knat1^{bp-9}* and *stm-GK*, respectively. Importantly, neither of the mutants reached the same level of xylem II formation at the end of their life cycle (10 weeks after germination). Hence, the mutants could not compensate later initiation of fiber differentiation by a later cessation of fiber production.

Redundant function of *KNAT1* and *STM* on xylem fiber differentiation

KNAT1 expression levels and patterns were unaltered in hypocotyls of *stm-GK*, whereas in *knat1^{bp-9}*, *STM* transcript abundance was mildly but significantly reduced to 66% of the expression level in wild type ($P<0.05$; Fig. 6F; supplementary material Fig. S7). In order to test whether *KNAT1* function is required for *STM* expression, we introgressed *knat1^{bp-1}*, a *knat1*-null mutation (dela Paz et al., 2012), into the *Col-0* background (referred to as *knat1^{bp-1C}*). In *knat1^{bp-1C}* hypocotyls, *STM* expression was more strongly reduced to 30% of the wild-type level than in *knat1^{bp-9}*, but not entirely abolished. This indicates that *STM* expression depends partially on *KNAT1* activity. However, because in *stm-GK*, which showed a less pronounced xylem phenotype than both *knat1^{bp-1C}* and *knat1^{bp-9}*, *STM* expression is reduced by more than two orders of magnitude (Fig. 6F), the effects of *KNAT1* on fiber differentiation are unlikely to be mediated solely through *STM*.

In a severely dwarfed double mutant of the weak *stm-GK* and *knat1^{bp-9}* alleles (supplementary material Fig. S1B, Fig. S2A and Fig. S8), xylem fiber differentiation was completely abolished (Fig. 6A–D), indicating that *STM* and *KNAT1* are redundantly required for xylem fiber differentiation. In comparison with the single mutants, radial xylem increment and transverse luminal area of vessel cells were synergistically reduced in hypocotyls of *stm-GK;knat1^{bp-9}*

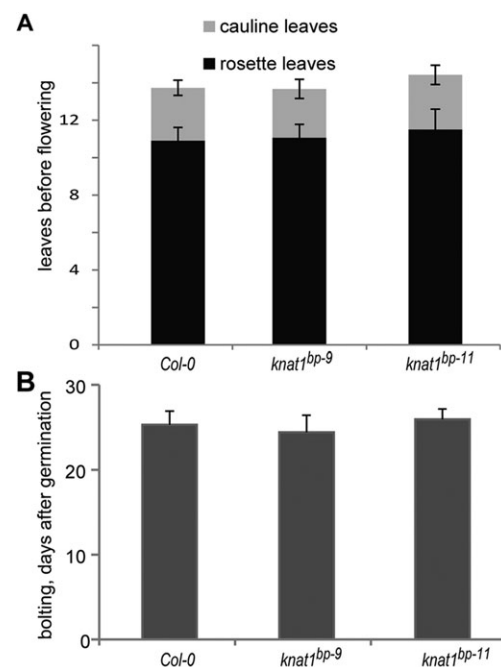


Fig. 5. *KNAT1* acts on xylem fiber differentiation independently of flowering time. (A,B) Flowering time expressed as the number of cauline and rosette leaves (A) or as days to bolting after germination (B) is not affected in *knat1* mutants. *t*-test, $P>0.05$, data are mean \pm s.d. of $n=11$ (A) and $n=30$ (B) biological replicates.

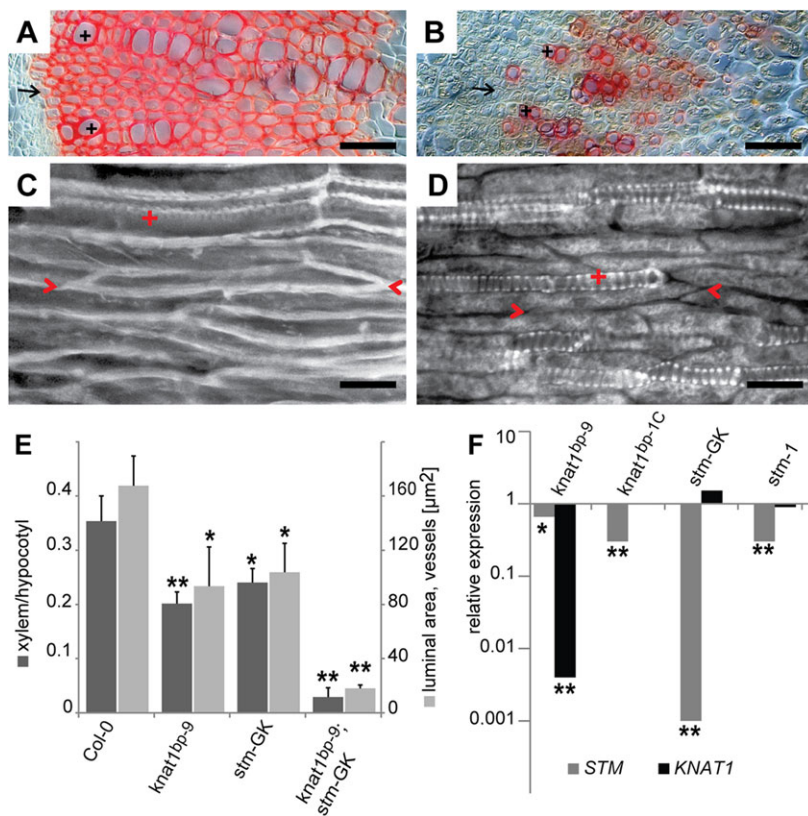


Fig. 6. Redundant function of *KNAT1* and *STM* on xylem fiber differentiation. (A–D) Phloroglucinol-stained transverse (A,B) and tangential (C,D) sections. (A,C) Wild type; (B,D) *knat1^{bp-9};stm-GK*. Red stain depicts lignified secondary cell walls (A,B). Arrows, xylem fiber cell file; +, neighboring xylem vessel cells; arrowheads, tip of xylem fiber. In *knat1^{bp-9};stm-GK*, walls of cells between vessel cells are not lignified. (E) Xylem expansion and luminal transverse area of xylem vessels are synergistically affected in *knat1^{bp-9};stm-GK*. Data are mean \pm s.d. of three independent experiments. * P <0.01; ** P <0.001, t -test; comparing mutants with wild type. (F) *KNAT1* is required for *STM* expression. qRT-PCR experiments employed RNA from three different independent experiments. *STM* expression is reduced in *knat1* mutants. Expression relative to *ACT2* and normalized to expression in Col-0 (=1). * P <0.05; ** P <0.01, t -test; comparing mutants with wild type. Scale bars: 50 μm in A,B; 20 μm in C,D.

(Fig. 6E). However, residual cambial activity and radial organization of cambial cell files were still retained in the double mutant (Fig. 6B), suggesting that meristem activity and maintenance are less sensitive to reduced *KNAT1* and *STM* function than fiber differentiation. In accordance with this, *WOX4* and *PXY/TDR*, which are associated with cambial activity, showed either increased or unaltered expression in 6-week-old hypocotyls of the double mutant, whereas *ATHB8* was less strongly expressed than in wild type (Fig. 7A). Importantly, transcript levels of xylem fiber identity genes *SND1* and *NST1*, and their downstream target *SND2* (Wang and Dixon, 2012), were all very strongly reduced in hypocotyls of *stm-GK;knat1^{bp-9}*. By contrast, the expression level of the phloem pole marker *APL* (Bonke et al., 2003) was not altered, and the expression of the vessel identity gene *VND7* (Wang and Dixon, 2012) was increased in the double mutant.

We then tested whether *KNAT1* and *STM* are co-expressed with SCW genes. Among the 100 most highly co-expressed genes of *KNAT1* and *STM* across a collection of more than 300 microarrays (Expression Angler) (Toufighi et al., 2005), 52 genes were co-expressed with both *STM* and *KNAT1*. Strikingly, among these 52 co-regulated genes we found 20 members of the 44 genes that make up the SCW regulon described by Persson et al. (2005) (supplementary material Table S1). We tested whether *KNAT1* and *STM* act upstream of the SCW regulon by performing qRT-PCR on 6-week-old hypocotyls of *stm-GK* and *knat1^{bp-9}*, as well as on the respective double mutant. *Cellulose synthase A (CESA) 4*, *CESA7* and *CESA8*, which are specific for SCW synthesis (Taylor et al., 2003), were significantly less strongly expressed in *knat1^{bp-9}* than in wild type (Fig. 7B). Partial removal of *STM* function in the *knat1^{bp-9}* background (i.e. in *stm-GK;knat1^{bp-9}*) reduced their transcript levels by more than two orders of magnitude. By contrast, five of the six *CESA* genes, which are specifically required for cellulose synthesis during primary wall formation (Persson et al., 2007; Sullivan et al., 2011), were not differentially expressed in *knat1^{bp-9};stm-GK*.

Together, these results suggest that *STM* and *KNAT1* are redundantly required for the expression of secondary wall genes but are not involved in cellulose deposition during primary growth.

KNAT1* and *STM* regulate xylem fiber differentiation through transcriptional repression of *BOP1* and *BOP2

Opposing functions of *STM* and *KNAT1* in the cambium, when compared with their functions in the SAM, could be due to differential, meristem-specific expression of genetic interactors. *BLADE-ON-PETIOLE1 (BOP1)* and *BOP2*, which encode BTB/POZ domain and ankyrin repeat-containing proteins (Norberg et al., 2005; Hepworth et al., 2005), antagonize the effect of *KNAT1* on pedicel angle in the *Arabidopsis* inflorescence stem and overexpression of *BOP1* and *BOP2* phenocopies the premature lignification phenotype of *knat1* mutant stems (Khan et al., 2012). We tested whether *BOP1* and *BOP2*, which are not expressed in the summit of the SAM, have a function in the cambium. Shortly after the onset of cambial activity, in 2-week-old hypocotyls, *pBOP1::GUS* was expressed in the cortex but was absent from the inner tissues (supplementary material Fig. S9A). At this stage, *pBOP2::GUS* was expressed in a reciprocal pattern, namely in the periderm, phloem, cambial zone and xylem (supplementary material Fig. S9B). In 3-week-old hypocotyls, *pBOP1::GUS* activity was no longer detectable in transverse sections of the hypocotyl (Fig. 8A), whereas *pBOP2::GUS* was strongest in the cambial zone and in the developing phloem, similar to *pKNAT1::GUS*, but notably absent from the developing xylem and mature xylem fibers (Fig. 8C). In the *knat1^{bp-1C}*-null mutant background, both *pBOP1::GUS* and *pBOP2::GUS* were overexpressed and, interestingly, *BOP2* expression occurred ectopically in xylem parenchyma cells (Fig. 8A–D). qRT-PCR confirmed that *BOP1* and *BOP2* were strongly de-repressed in *knat1^{bp-1C}* and to a lesser extent in *stm-1^C* (*stm-1* introgressed into Col-0) hypocotyls (Fig. 8G), suggesting that

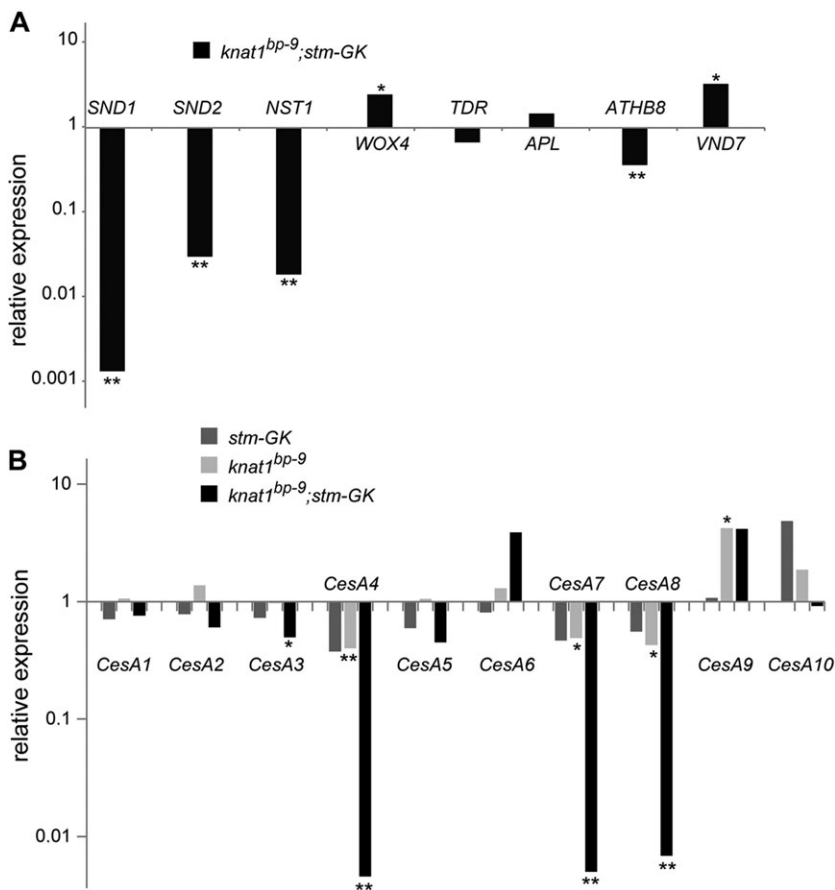


Fig. 7. *KNAT1* and *STM* regulate secondary wall genes.

(A,B) qRT-PCR experiments. (A) Gene expression of cambial marker genes in *knat1^{bp-9};stm-GK*. Expression of the fiber marker genes *SND1* and *NST1* was strongly reduced in *knat1^{bp-9};stm-GK*. (B) Gene expression of cellulose synthases involved in secondary cell wall deposition is globally reduced in *knat1^{bp-9};stm-GK*. Cellulose synthases *CesA4*, *CesA7* and *CesA8* are specifically involved in secondary cell wall deposition. (A,B) qRT-PCR experiments employed RNA from three different independent experimental replicates. Data represent averages of experimental replicates. Expression is relative to *ACT2* and normalized to expression in Col-0 (=1). * $P < 0.05$; ** $P < 0.01$, *t*-test.

KNAT1 and *STM* act upstream of *BOP1* and *BOP2*. By contrast, we did not observe any change in gene expression levels of *KNAT1* and *STM* in a *bop1;bop2* double mutant (Fig. 8E-G), indicating that negative regulation of *KNAT1* expression by *BOP1* and *BOP2*, as occurs in the embryonic hypocotyl (Jun et al., 2010), is no longer active during later stages of hypocotyl development.

In order to test whether BOP genes are of functional importance during secondary xylem formation and whether ectopic BOP expression in xylem parenchyma could explain the *knat1* fiber phenotype, we analyzed a *bop1;bop2* double mutant. *bop1;bop2* hypocotyls displayed increased xylem fiber formation, whereas ectopic expression of *BOP1* led to an opposite phenotype and was sufficient to prevent xylem fiber differentiation to a similar degree as in strong *knat1* mutants (Fig. 8H-L). Furthermore, the *knat1^{bp-1C}* fiber differentiation phenotype, but not the reduced cambial activity, was completely suppressed by *bop1;bop2* (Fig. 8I-M; supplementary material Fig. S10), indicating that *KNAT1* acts on fiber differentiation independently of cambial activity through the repression of BOP genes. Ectopic BOP expression in xylem parenchyma is therefore likely to account for repression of xylem fiber differentiation in *knat1* mutants.

DISCUSSION

The simple anatomy of the cambium in *Arabidopsis* hypocotyls and the use of weak loss-of-function mutant alleles permitted us to uncover a promotive function of *KNAT1* and *STM* on xylem differentiation, a yet unknown role that is in sharp contrast with their suggested inhibitory mode-of-action on cell differentiation in the SAM. Although there is a large body of evidence to indicate that *STM* and *KNAT1* repress differentiation in the SAM, conclusions

about the functions of these genes were often based on spectacular phenotypes resulting from ectopic overexpression of class I KNOX genes, typically leading to adventitious meristems and highly lobed leaf margins (Hay and Tsiantis, 2010). Little attention has been given to evidence challenging the view of *STM* and *KNAT1* being simply repressors of differentiation. For example, the recessive *waldmeister* (*stm^{wam}*) mutant shows fasciated inflorescences and delayed senescence (Felix et al., 1996) characteristics, which are not consistent with the proposed repressive function of *STM* on differentiation. Additionally, *stm^{gorgon}*, a partial loss-of-function mutant, displays fasciated shoot apical and inflorescence meristems (Takano et al., 2010), resulting in a shoot architecture reminiscent of *clavata* mutants. *CLV3* transcript levels, which are reduced in the nonsense mutant *stm-1*, and *WUS* are increased in *stm^{gorgon}* (Takano et al., 2010). As *stm^{gorgon}* is a recessive hypomorphic mutation it seems likely that different levels of STM activity can have different, even opposite, effects. In the hypocotyl, however, strong *stm* mutants, which did not establish a SAM, had a similar, although more pronounced, xylem phenotype compared with weak *stm* mutants. Notably, in both weak and strong mutants of *stm* and *knat1*, cambial growth was retained. Thus, rather than being the result of different STM or KNAT1 levels in the SAM versus the cambium, the apparently opposite consequences of reduced levels of *STM* and *KNAT1* between the two types of meristems are likely caused by a different mechanism. Similar *STM* and *KNAT1* expression levels in inflorescence meristems and the cambium (Fig. 1) are in keeping with this conclusion.

Spicer and Groover (2010) proposed that regulators of meristem maintenance and activity from the SAM have been co-opted during the evolution of cambia. As different *WUS* and *CLV3* paralogs

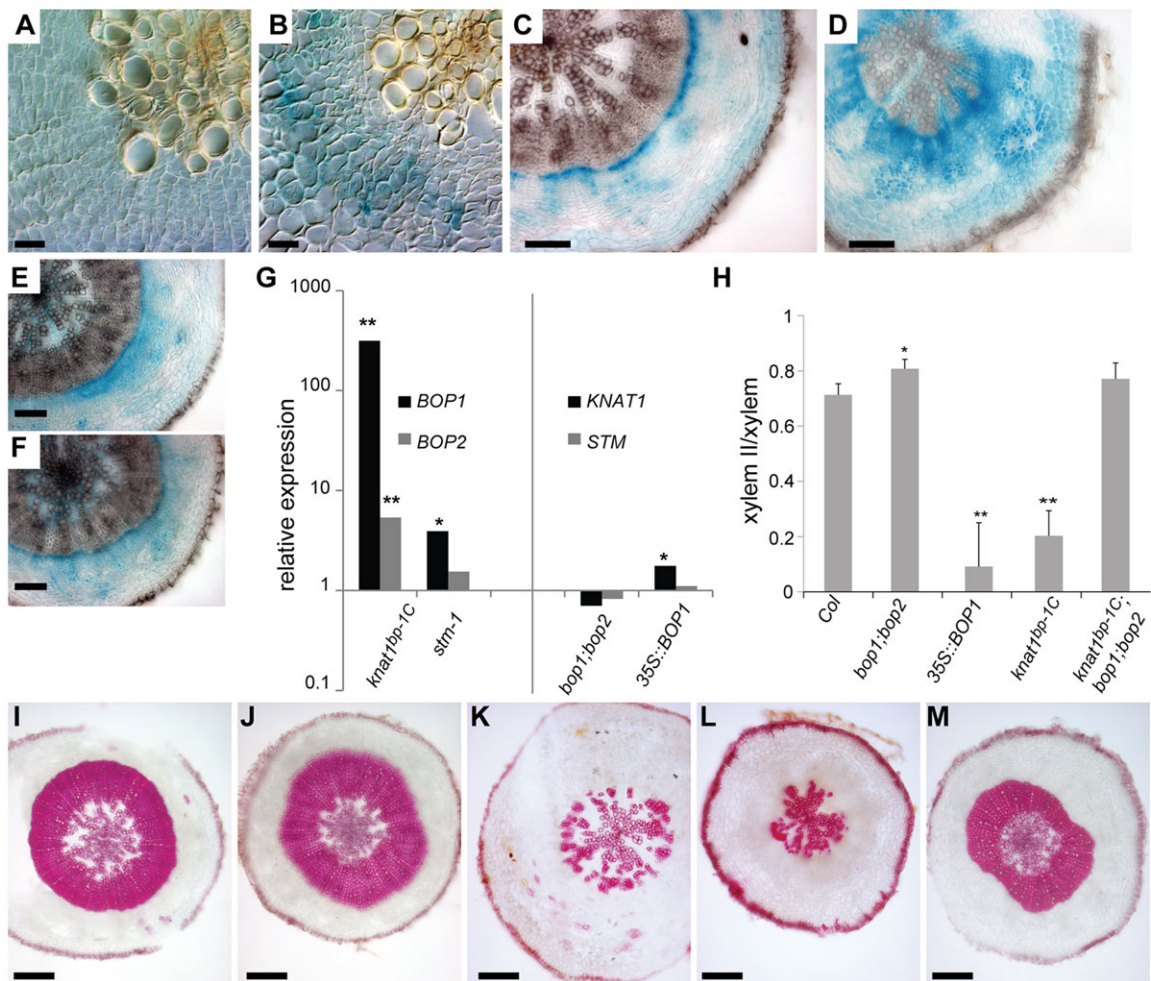


Fig. 8. *KNAT1* and *STM* regulate xylem fiber differentiation through *BOP1* and *BOP2*. (A–F) GUS reporter activity in transverse sections of 3-week-old (A, B) and 5-week-old (C–F) hypocotyls. (A) *pBOP1::GUS*; (B) *pBOP1::GUS; knat1^{bp-1C}*; (C) *pBOP2::GUS*; (D) *pBOP2::GUS; knat1^{bp-1C}*; (E) *pKNAT1::GUS*; (F) *pKNAT1::GUS; bop1;bop2*. (G) qRT-PCR experiments employed RNA of 4-week-old hypocotyls from three different independent experimental replicates. Data represent averages of experimental replicates. Expression is relative to *ACT2* and normalized to expression in Col-0 (=1). (H) Ratio between the area occupied by xylem II and total xylem in transverse sections from 6-week-old hypocotyls. Data are mean±s.d. of three independent experiments per genotype, with three hypocotyls per experiment. (G, H) * $P < 0.05$; ** $P < 0.01$, *t*-test comparing mutants with wild type. (I–M) Phloroglucinol staining of 6-week-old hypocotyls: (I) wild type (Col-0); (J) *bop1;bop2*; (K) *35S::BOP1*; (L) *knat1^{bp-1C}*; (M) *knat1^{bp-1C}; bop1;bop2*. Scale bars: 20 μ m in A, B; 100 μ m in C–F; 200 μ m in I–M.

govern meristem regulation in apical and lateral meristems, neo-functionalization of *WUS* and *CLV* paralogs may have only required divergence in their promoter but not protein-coding sequences. Recruitment of class I KNOX genes from apical to lateral meristem regulators would have required an expansion of their expression domain to the cambium but did not involve gene duplication. Divergent functions of *STM* and *KNAT1* between different types of meristems could be the result of meristem type-specific transactivation targets, due to different chromatin structures, to genetic or protein-protein interactions, or to concentration-dependent binding to a different suite of promoters.

As class I KNOX genes are present in the moss *Physcomitrella patens* (Sakakibara et al., 2008), a non-vascular plant that lacks a functional xylem, lignified xylem fibers and a cambium, their ancestral function cannot be specific to cambia and their role might be of a more general nature, e.g. promoting cell division. In seedlings of strong *stm* mutants, meristem-like structures occur in the axils of cotyledons, which are much smaller than the wild-type SAM and comprise only slightly enlarged cells (Endrizzi et al., 1996; Barton and Poethig, 1993). This suggests that in the SAM,

STM is required for cell division and has only limited effects on the repression of differentiation. By contrast, our results show that, in the cambium, cell proliferation is less sensitive to reduced *KNAT1* and *STM* levels than cell differentiation. We suggest that in the cambium at sites of high class I KNOX activity, cell proliferation overrides the simultaneously induced differentiation mediated by repression of BOP expression. Conversely, in the expansion zone, *STM* and *KNAT1* activity may drop below a threshold required for cell proliferation that is, however, still sufficient to repress BOP expression and as a consequence allow differentiation. By contrast, due to the absence of *BOP1* and *BOP2* expression from the center of the SAM (Norberg et al., 2005), rather than due to an effect on cell differentiation, reduced *STM* and *KNAT1* function would only affect cell division activity in the SAM. In line with this hypothesis, no SAM phenotype has been reported for recessive BOP mutants to date. Rather than meristem type-specific access to a different suite of promoters, the discrepancy between the SAM and cambium phenotype of *stm* and *knat1* mutants could therefore be a consequence of differential expression of BOP genes.

MATERIALS AND METHODS

Plant material

Plants were grown under standard greenhouse conditions on soil with 16 h light per day and at 23°C. Unless otherwise stated, hypocotyls were dissected 6 weeks after germination, which corresponded to the onset of senescence of the first silique. Hypocotyls were cut basal to the petioles of the cotyledons and 3 mm long segments (rootward) were employed for anatomical analyses and RNA extractions. KNOX mutants were purchased from the *Arabidopsis* Stock Centre, Nottingham, UK. Accession numbers and primers used for genotyping can be found in supplementary material Tables S2 and S3.

Anatomy

Phloroglucinol staining was performed on hand sections or 30 µm vibratome sections. For vibratome sections, hypocotyls were embedded in 5% agarose. The sections were incubated in 70% ethanol for 1 min and then directly transferred to phloroglucinol (in 20% HCl) for 3 min. Sections were mounted on glass slides in chloral hydrate:glycerol:H₂O (8:3:1) clearing solution. For imaging, an AxioCam mounted on an AxioPlan 2 stereomicroscope (Zeiss) was used. The Axiovision 4.8 software was employed to measure sizes and areas.

GUS stainings were performed on freshly harvested hypocotyl segments of 3 mm length. The segments were immediately immersed in GUS staining solution (Fischer et al., 2006) and placed on ice. After vacuum infiltration of the staining solution, hypocotyls were incubated at 37°C on a shaker for 3 h. Subsequently, the tissue was fixed in FAE (2% formaldehyde, 5% acetic acid, 63% ethanol) for 1 h and stored in 70% ethanol. For microscopy, GUS-stained hypocotyls were hand sectioned, mounted and observed as the phloroglucinol stained samples.

For Toluidine Blue staining, hypocotyls were fixed in FAE for 1 h and then dehydrated in an ethanol, isopropanol, Roti-Histol (Roth Laborbedarf, Germany) concentration series and embedded in paraffin (Rotiplast, Roth Laborbedarf) (Escalante-Pérez et al., 2009). Blocks were sectioned into 30 µm sections using a sliding microtome (Reichert, Austria). After removal of the paraffin with xylene, sections were stained in 1% Toluidine Blue O (TBO, Sigma) for 1 min.

Gene expression analyses

Total RNA was isolated from freshly harvested hypocotyls or other tissues using the RNeasy Plant Mini Kit (Qiagen) following the manufacturer's guidelines. Prior to first-strand cDNA synthesis (QuantiTect Reverse Transcription, Qiagen) the Ambion Turbo DNase kit (Invitrogen) was employed to remove residual gDNA. Total RNA (1 µg) was used for first-strand cDNA synthesis. qRT-PCR was carried out using the ROCHE LightCycler480 SYBR Green I Master kit (Roche) and reactions were run on a LightCycler 480 (Roche) with preincubation at 95°C for 5 min; and amplification cycles of 95°C for 10 s, 61°C for 10 s and 72°C for 10 s. Data were analyzed using LightCycler 480 Software Release 1.5.0 (Roche). Amplification efficiencies were calculated with the help of cDNA dilution series and relative expression values were calculated according to Pfaffl (2001). ACTIN2 expression was used as an internal standard. Primers are listed in supplementary material Table S3.

Immunohistochemistry

For immunolocalization with the monoclonal rat JIM13 antibody (Complex Carbohydrate Research Center, CCRC, University of Georgia, Athens, GA, USA), hypocotyls were fixed in 4% formaldehyde in 1× PME (100 mM PIPES, 1 mM MgSO₄, 2 mM EGTA) and 30 µm vibratome sections were cut. BSA (5%) was used for blocking. Primary and secondary [Alexa Fluor 568 goat anti-rat IgG (H+L), Life Technologies] antibodies were diluted 1:40 and 1:300, respectively. After immunolabeling, sections were counterstained with calcofluor white (0.001%). Images were acquired with a Zeiss LSM780 confocal microscope with 405 nm excitation and 415–445 nm emission for calcofluor white, and 561 nm excitation and 575–600 nm emission for the secondary antibody.

Micrografting

Grafting was carried out between scions and stocks of hypocotyls as described previously (Turnbull et al., 2002) using 5-day-old seedlings

grown on 1/2 MS plates at 24°C with 16 h light per day. Pieces of silicon tubes (3–5 mm) were used during grafting. Successful grafts were transferred into soil 5 days after grafting and grown under 16 h light conditions at 23°C. Hypocotyls were sampled when plants were 6 weeks old.

Acknowledgements

We thank Angela Hay (University of Oxford, UK) and Wolfgang Werr (University of Cologne, Germany) for providing us with *knat1^{bp-9}* and *pSTM::GUS* seed stocks, respectively. We also thank Björn Sundberg for constructive discussions and advice.

Competing interests

The authors declare no competing financial interests.

Author contributions

D.L., W.S., M.H., M.N., J.Z., H.C.H., H.H., X.J. and U.F. performed and analyzed the experiments. Y.H., O.N., A.P. and U.F. designed the research and edited the manuscript. D.L., W.S. and U.F. wrote the manuscript.

Funding

This work was funded by Bio4Energy (U.F.), Plant Fellows (European Union's 7th Framework Programme, GA-2010-267243 to D.L.), the Berzelii Centre (O.N.), Deutsche Forschungsgemeinschaft 'Pappelgruppe' (A.P.), and by the Academy of Finland, TEKES and European Research Council 'Advanced Investigator Grant' (Y.H.).

Supplementary material

Supplementary material available online at <http://dev.biologists.org/lookup/suppl/doi:10.1242/dev.111369/-DC1>

References

- Aichinger, E., Kornet, N., Friedrich, T. and Laux, T. (2012). Plant stem cell niches. *Annu. Rev. Plant Biol.* **63**, 615–636.
- Baima, S., Nobili, F., Sessa, G., Lucchetti, S., Ruberti, I. and Morelli, G. (1995). The expression of the Athb-8 homeobox gene is restricted to provascular cells in *Arabidopsis thaliana*. *Development* **121**, 4171–4182.
- Barton, M. K. and Poethig, R. S. (1993). Formation of the shoot apical meristem in *Arabidopsis thaliana* - an analysis of development in the wild-type and in the shoot meristemless mutant. *Development* **119**, 823–831.
- Bonke, M., Thitamadee, S., Mähönen, A. P., Hauser, M.-T. and Helariutta, Y. (2003). APL regulates vascular tissue identity in *Arabidopsis*. *Nature* **426**, 181–186.
- Brand, U., Fletcher, J. C., Hobe, M., Meyerowitz, E. M. and Simon, R. (2000). Dependence of stem cell fate in *Arabidopsis* on a feedback loop regulated by CLV3 activity. *Science* **289**, 617–619.
- Busse, J. S. and Evert, R. F. (1999). Vascular differentiation and transition in the seedling of *Arabidopsis thaliana* (Brassicaceae). *Int. J. Plant Sci.* **160**, 241–251.
- Byrne, M. E., Simorowski, J. and Martienssen, R. A. (2002). ASYMMETRIC LEAVES1 reveals knox gene redundancy in *Arabidopsis*. *Development* **129**, 1957–1965.
- Chaffey, N., Cholewa, E., Regan, S. and Sundberg, B. (2002). Secondary xylem development in *Arabidopsis*: a model for wood formation. *Physiol. Plant* **114**, 594–600.
- Cuny, H. E., Rathgeber, C. B. K., Frank, D., Fonti, P. and Fournier, M. (2014). Kinetics of tracheid development explain conifer tree-ring structure. *New Phytol.* **203**, 1231–1241.
- dela Paz, J. S., Stronghill, P. E., Douglas, S. J., Saravia, S., Hasenkamp, C. A. and Riggs, C. D. (2012). Chromosome fragile sites in *Arabidopsis* harbor matrix attachment regions that may be associated with ancestral chromosome rearrangement events. *PLoS Genet.* **8**, e1003136.
- Endrizzi, K., Moussian, B., Haecker, A., Levin, J. Z. and Laux, T. (1996). The SHOOT MERISTEMLESS gene is required for maintenance of undifferentiated cells in *Arabidopsis* shoot and floral meristems and acts at a different regulatory level than the meristem genes WUSCHEL and ZWILLE. *Plant J.* **10**, 967–979.
- Escalante-Pérez, M., Lautner, S., Nehls, U., Selle, A., Teuber, M., Schnitzler, J. P., Teichmann, T., Fayyaz, P., Hartung, W., Polle, A. et al. (2009). Salt stress affects xylem differentiation of grey poplar (*Populus×canescens*). *Planta* **229**, 299–309.
- Felix, G., Altmann, T., Uwer, U., Jessop, A., Willmitzer, L. and Morris, P.-C. (1996). Characterization of *waldmeister*, a novel developmental mutant in *Arabidopsis thaliana*. *J. Exp. Bot.* **47**, 1007–1017.
- Fischer, U., Ikeda, Y., Ljung, K., Serralbo, O., Singh, M., Heidstra, R., Palme, K., Scheres, B. and Grebe, M. (2006). Vectorial information for *Arabidopsis* planar polarity is mediated by combined AUX1, EIN2, and GNOM activity. *Curr. Biol.* **16**, 2143–2149.
- Gardiner, J., Donner, T. J. and Scarpella, E. (2011). Simultaneous activation of SHR and ATHB8 expression defines switch to preprocambial cell state in *Arabidopsis* leaf development. *Dev. Dyn.* **240**, 261–270.

- Groover, A. T., Mansfield, S. D., DiFazio, S. P., Dupper, G., Fontana, J. R., Millar, R. and Wang, Y. (2006). The Populus homeobox gene ARBORKNOX1 reveals overlapping mechanisms regulating the shoot apical meristem and the vascular cambium. *Plant Mol. Biol.* **61**, 917-932.
- Hall, H. C., Cheung, J. and Ellis, B. E. (2013). Immunoprofiling reveals unique cell-specific patterns of wall epitopes in the expanding Arabidopsis stem. *Plant J.* **74**, 134-147.
- Hay, A. and Tsiantis, M. (2010). KNOX genes: versatile regulators of plant development and diversity. *Development* **137**, 3153-3165.
- Hepworth, S. R., Zhang, Y., McKim, S., Li, X. and Haughn, G. W. (2005). BLADE-ON-PETIOLE-dependent signaling controls leaf and floral patterning in Arabidopsis. *Plant Cell* **17**, 1434-1448.
- Hirakawa, Y., Kondo, Y. and Fukuda, H. (2010). TDIF peptide signaling regulates vascular stem cell proliferation via the WOXA homeobox gene in Arabidopsis. *Plant Cell* **22**, 2618-2629.
- Jasinski, S., Piazza, P., Craft, J., Hay, A., Woolley, L., Rieu, I., Phillips, A., Hedden, P. and Tsiantis, M. (2005). KNOX action in Arabidopsis is mediated by coordinate regulation of cytokinin and gibberellin activities. *Curr. Biol.* **15**, 1560-1565.
- Jun, J. H., Ha, C. M. and Fletcher, J. C. (2010). BLADE-ON-PETIOLE1 coordinates organ determinacy and axial polarity in Arabidopsis by directly activating ASYMMETRIC LEAVES2. *Plant Cell* **22**, 62-76.
- Khan, M., Xu, M., Murmu, J., Tabb, P., Liu, Y., Storey, K., McKim, S. M., Douglas, C. J. and Hepworth, S. R. (2012). Antagonistic interaction of BLADE-ON-PETIOLE1 and 2 with BREVIPEDICELLUS and PENNYWISE regulates Arabidopsis inflorescence architecture. *Plant Physiol.* **158**, 946-960.
- Lenhard, M., Jurgens, G. and Laux, T. (2002). The WUSCHEL and SHOOTMERISTEMLESS genes fulfil complementary roles in Arabidopsis shoot meristem regulation. *Development* **129**, 3195-3206.
- Lincoln, C., Long, J., Yamaguchi, J., Serikawa, K. and Hake, S. (1994). A knotted1-like homeobox gene in Arabidopsis is expressed in the vegetative meristem and dramatically alters leaf morphology when overexpressed in transgenic plants. *Plant Cell* **6**, 1859-1876.
- Long, J. A. and Barton, M. K. (1998). The development of apical embryonic pattern in Arabidopsis. *Development* **125**, 3027-3035.
- Mele, G., Ori, N., Sato, Y. and Hake, S. (2003). The knotted1-like homeobox gene BREVIPEDICELLUS regulates cell differentiation by modulating metabolic pathways. *Genes Dev.* **17**, 2088-2093.
- Norberg, M., Holmlund, M. and Nilsson, O. (2005). The BLADE ON PETIOLE genes act redundantly to control the growth and development of lateral organs. *Development* **132**, 2203-2213.
- Persson, S., Wei, H., Milne, J., Page, G. P. and Somerville, C. R. (2005). Identification of genes required for cellulose synthesis by regression analysis of public microarray data sets. *Proc. Natl. Acad. Sci. USA* **102**, 8633-8638.
- Persson, S., Paredes, A., Carroll, A., Palsdottir, H., Doblin, M., Poindexter, P., Khitrov, N., Auer, M. and Somerville, C. R. (2007). Genetic evidence for three unique components in primary cell-wall cellulose synthase complexes in Arabidopsis. *Proc. Natl. Acad. Sci. USA* **104**, 15566-15571.
- Pfaffl, M. W. (2001). A new mathematical model for relative quantification in real-time RT-PCR. *Nucleic Acids Res.* **29**, e45.
- Ragni, L. and Hardtke, C. S. (2013). Small but thick enough - the Arabidopsis hypocotyl as a model to study secondary growth. *Physiol. Plant.* **51**, 164-171.
- Ragni, L., Belles-Boix, E., Gunl, M. and Pautot, V. (2008). Interaction of KNAT6 and KNAT2 with BREVIPEDICELLUS and PENNYWISE in Arabidopsis inflorescences. *Plant Cell* **20**, 888-900.
- Ragni, L., Nieminen, K., Pacheco-Villalobos, D., Sibout, R., Schwechheimer, C. and Hardtke, C. S. (2011). Mobile gibberellin directly stimulates Arabidopsis hypocotyl xylem expansion. *Plant Cell* **23**, 1322-1336.
- Sakakibara, K., Nishiyama, T., Deguchi, H. and Hasebe, M. (2008). Class 1 KNOX genes are not involved in shoot development in the moss *Physcomitrella patens* but do function in sporophyte development. *Evol. Dev.* **10**, 555-566.
- Sanchez, P., Nehlin, L. and Greb, T. (2012). From thin to thick: major transitions during stem development. *Trends Plant Sci.* **17**, 113-121.
- Schoof, H., Lenhard, M., Haecker, A., Mayer, K. F. X., Jürgens, G. and Laux, T. (2000). The stem cell population of Arabidopsis shoot meristems is maintained by a regulatory loop between the CLAVATA and WUSCHEL genes. *Cell* **100**, 635-644.
- Schrader, J., Nilsson, J., Mellerowicz, E., Berglund, A., Nilsson, P., Hertzberg, M. and Sandberg, G. (2004). A high-resolution transcript profile across the wood-forming meristem of poplar identifies potential regulators of cambial stem cell identity. *Plant Cell* **16**, 2278-2292.
- Schuetz, M., Smith, R. and Ellis, B. (2013). Xylem tissue specification, patterning, and differentiation mechanisms. *J. Exp. Bot.* **64**, 11-31.
- Scotfield, S., Dewitte, W., Nieuwland, J. and Murray, J. A. H. (2013). The Arabidopsis homeobox gene SHOOT MERISTEMLESS has cellular and meristem-organizational roles with differential requirements for cytokinin and CYCD3 activity. *Plant J.* **75**, 53-66.
- Shi, C.-L., Stenvik, G.-E., Vie, A. K., Bones, A. M., Pautot, V., Proveniers, M., Aalen, R. B. and Butenko, M. A. (2011). Arabidopsis class I KNOTTED-like homeobox proteins act downstream in the IDA-HAE/HSL2 floral abscission signaling pathway. *Plant Cell* **23**, 2553-2567.
- Sibout, R., Plantegenet, S. and Hardtke, C. S. (2008). Flowering as a condition for xylem expansion in Arabidopsis hypocotyl and root. *Curr. Biol.* **18**, 458-463.
- Skene, D. S. (1969). Period of time taken by cambial derivatives to grow and differentiate into tracheids in *Pinus radiata*. *Ann. Bot.* **33**, 253.
- Spicer, R. and Groover, A. (2010). Evolution of development of vascular cambia and secondary growth. *New Phytol.* **186**, 577-592.
- Stahl, Y., Wink, R. H., Ingram, G. C. and Simon, R. (2009). A signaling module controlling the stem cell niche in Arabidopsis root meristems. *Curr. Biol.* **19**, 909-914.
- Sullivan, S., Ralet, M.-C., Berger, A., Diatloff, E., Bischoff, V., Gonneau, M., Marion-Poll, A. and North, H. M. (2011). CESA5 is required for the synthesis of cellulose with a role in structuring the adherent mucilage of Arabidopsis seeds. *Plant Physiol.* **156**, 1725-1739.
- Takano, S., Niihama, M., Smith, H. M. S., Tasaka, M. and Aida, M. (2010). gorgon, a novel missense mutation in the SHOOT MERISTEMLESS gene, impairs shoot meristem homeostasis in Arabidopsis. *Plant Cell Physiol.* **51**, 621-634.
- Taylor, N. G., Howells, R. M., Huttly, A. K., Vickers, K. and Turner, S. R. (2003). Interactions among three distinct CesA proteins essential for cellulose synthesis. *Proc. Natl. Acad. Sci. USA* **100**, 1450-1455.
- Toufighi, K., Brady, S. M., Austin, R., Ly, E. and Provart, N. J. (2005). The botany array resource: e-northers, expression angling, and promoter analyses. *Plant J.* **43**, 153-163.
- Turnbull, C. G. N., Booker, J. P. and Leyser, H. M. O. (2002). Micrografting techniques for testing long-distance signalling in Arabidopsis. *Plant J.* **32**, 255-262.
- Wang, H.-Z. and Dixon, R. A. (2012). On-off switches for secondary cell wall biosynthesis. *Mol. Plant* **5**, 297-303.
- Yadav, R. K., Perales, M., Gruel, J., Girke, T., Jonsson, H. and Reddy, G. V. (2011). WUSCHEL protein movement mediates stem cell homeostasis in the Arabidopsis shoot apex. *Genes Dev.* **25**, 2025-2030.

Fig. S1. (A) qRT-PCR employing RNA of 6-week-old hypocotyls from three different independent experimental replicates. Bars represent averages of experimental replicates. Expression relative to *ACT2* and normalized to expression in Col-0 (= 1); **, $P < 0.01$, *t*-test; comparing mutants to wild type. (B) Aerial biomass of 6-week-old plants. *knat1^{bp-9}* and *stm-GK* accumulated the same amount of aerial biomass as wild type. Bars represent averages and standard deviations of three independent experiments (n = 3) with each three plants per genotype. *, $P < 0.05$; **, $P < 0.01$; *t*-test.

Fig. S2. (A) Dissected 6-week-old hypocotyls. Scale bar, 1mm. (B) transverse sections of 6-week-old hypocotyls. Scale bar: 300 μ m. (C) Ratio between the area occupied by xylem II and total xylem area in transverse sections from 6-week-old hypocotyls. Bars represent averages and standard deviations of three independent experiments per genotype, with each three hypocotyls per experiment.

Fig. S3. Vascular bundles of *knat1^{bp-9}* and *stm-GK* inflorescence stems are impaired in xylem fiber differentiation. Transverse 30 μ m sections of the oldest internode of 10-week-old plants are shown. Lignified cell walls appear in red, phloroglucinol stained. (B,C) White arrowheads point to bundles without lignified xylem fibers. Scale bars: 200 μ m (A,B); 500 μ m (C); 50 μ m (D-F). (A,D) Col-0; (B,E) *knat1^{bp-9}*; (C,F) *stm-GK*.

Fig. S4. Radial dimension of cambium-expansion zones, including the meristem. (A-F) Immunolabelling of JIM13 epitope, which marks mature phloem bundles and xylem vessels and fibers, in transverse sections of 3-week-old (A-C) and 4-week-old (D-F) hypocotyls. Cell walls counterstained with calcofluor white. Scale bars: 20 μ m. White arrowheads point to JIM13-positive phloem bundles; red arrowheads to mature xylem vessels and fibers. (A,D) Col-0; (B,E) *knat1^{bp-9}*; (C,F) *stm-GK*. (G) Size of cambium-expansion zone in radial direction between mature JIM13 positive phloem bundles and xylem fibers and vessels in 3-week-old and 4-week-old hypocotyls. Bars represent averages and standard deviations of three biological replicates*, $P < 0.05$; **, $P < 0.01$; *t*-test.

Fig. S5. Dissected 6-week-old hypocotyls from reciprocal grafting experiments. Arrowheads point to the grafting junction. (A) *Ler* scion on *Ler* stock; (B) *Ler* scion on *knat1^{bp-1}* stock; (C) *knat1^{bp-1}* scion on *Ler* stock; (D) *knat1^{bp-1}* scion on *knat1^{bp-1}* stock.

Fig. S6. (A) Time series of xylem II development. Data points represent averages and standard deviations of three biological replicates. (B-G) 30 μ m thick transverse sections of Col-0 (B,E) *knat1^{bp-9}* (C,F) and *stm-GK* (D,G). (B-D) Three weeks after germination; scale bars 100 μ m. (E-G) four weeks after germination. Scale bars: 50 μ m. Black arrowheads point to center of hypocotyls; white arrowheads to mature xylem fibers (E).

Fig. S7. *KNAT1* and *STM* promoter activity in *stm-GK*, or *knat1^{bp-9}* background, respectively. Details of the transition zone from cambium to phloem (bottom) and xylem (top), respectively, of transverse sections from 6-week-old hypocotyls after GUS staining. (A) p*KNAT1*::*GUS*; (B) p*KNAT1*::*GUS*, *stm-GK*; (C) p*STM*::*GUS*; (D) p*STM*::*GUS*, *knat1^{bp-9}*. Scale bars: 20 μ m. +, xylem vessel.

Fig. S8. 4-week-old Col-0 (A) and *knat1^{bp-9}*; *stm-GK* (B) plants. The double mutant is severely dwarfed with a reduced number of leaves. Scale bars: 10 mm.

Fig. S9. GUS stainings of 2-week-old hypocotyls. Transverse 30 μ m thick sections. Scale bars: 200 μ m. (A) p*BOP1*::*GUS*; (B) p*BOP2*::*GUS*; (C) p*KNAT1*::*GUS*.

Fig. S10. Reduced luminal areas of xylem parenchyma and fiber cells of *knat1^{bp-1}* are restored to wild-type size in *knat1^{bp-1}*; *bop1*; *bop2* independently of cambial activity. (A) Luminal areas. Data points

represent averages and standard deviations of three biological replicates. For each replicate and cell type luminal areas of 10 cells were measured. (B) Ratio between number of xylem fiber cells (xylem II) to total number of xylary cells in a cambial cell file. (C) Number of cells per cambial cell file. (B,C) Data points represent averages and standard deviations of three biological replicates. For each replicate cell counts of three cell files were determined. (A-C) *, $P < 0.05$; **, $P < 0.01$; t -test. mutants compared with wild type.

Table S1. Genes co-expressed with both *KNATI* and *STM*. The 100 most strongly co-expressed genes for each *KNATI* and *STM* were identified from a collection of more than 300 microarrays (Expression Angler; www.bar.utoronto.ca; Toufighi et al., 2004) and ranked in the order of decreasing r -values. Genes co-expressed with both *STM* and *KNATI* are listed according to the sum of their rankings ($\text{rank}(\textit{KNATI}) + \text{rank}(\textit{STM})$). Y, part of the SCW regulon according to Persson et al. (2005).

Table S2. Seed stocks.

Table S3. A list of primers used in this study.

Fig. S1

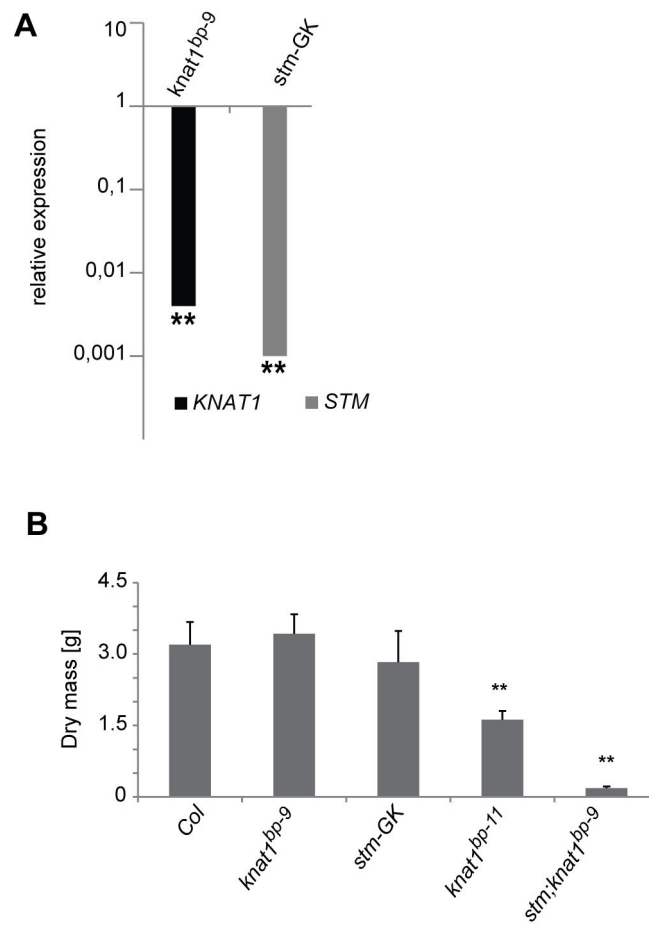


Fig. S2

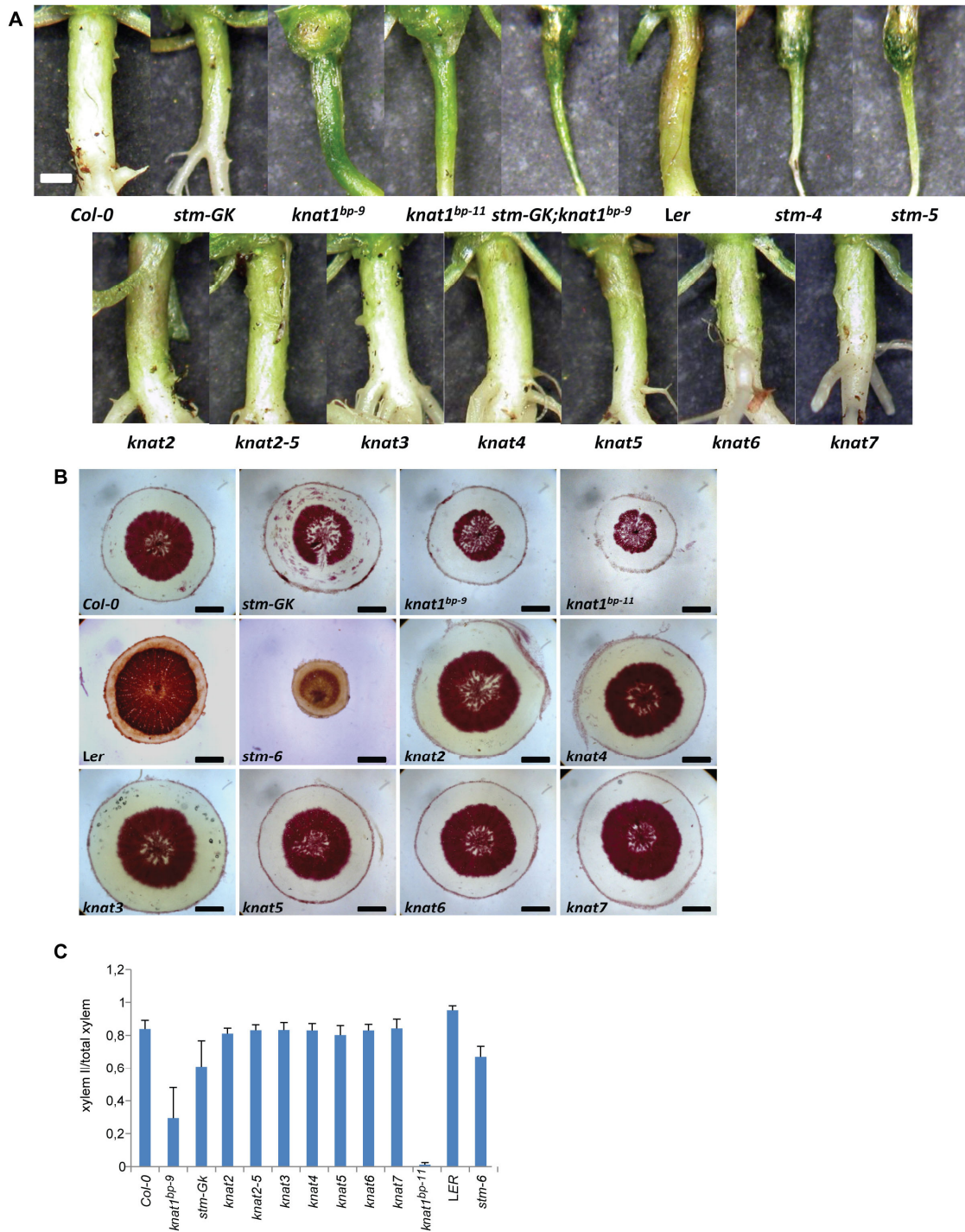


Fig. S3

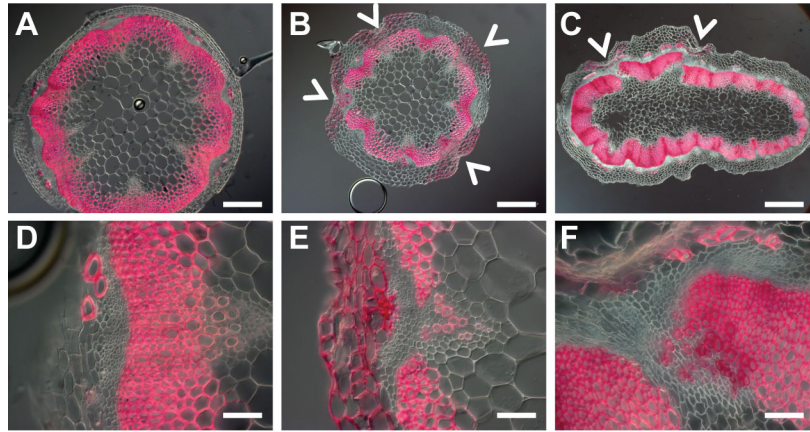


Fig. S4

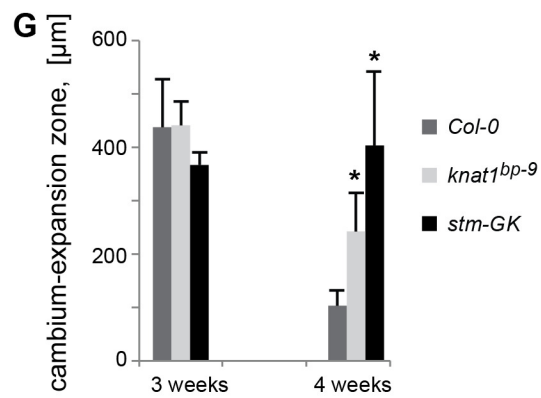
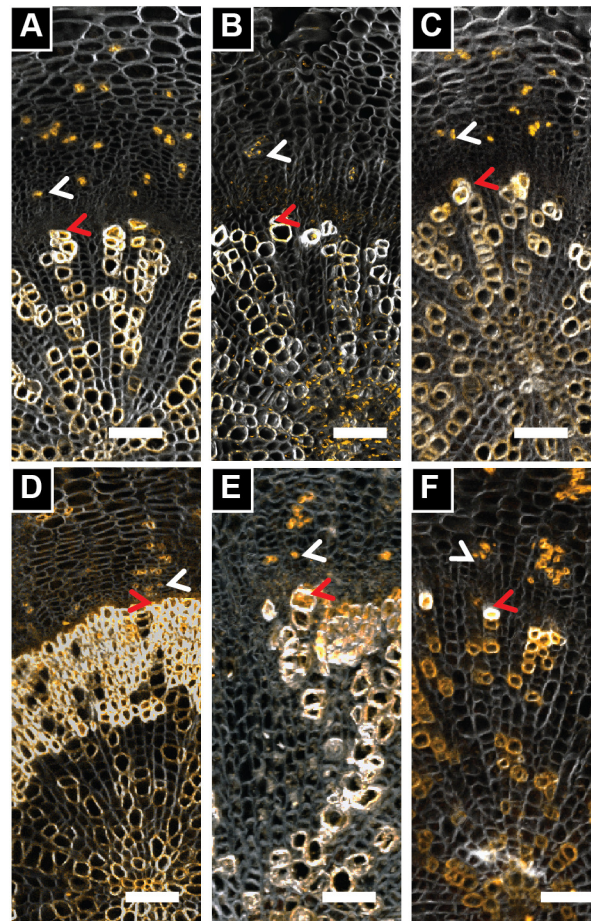


Fig. S5



Fig. S6

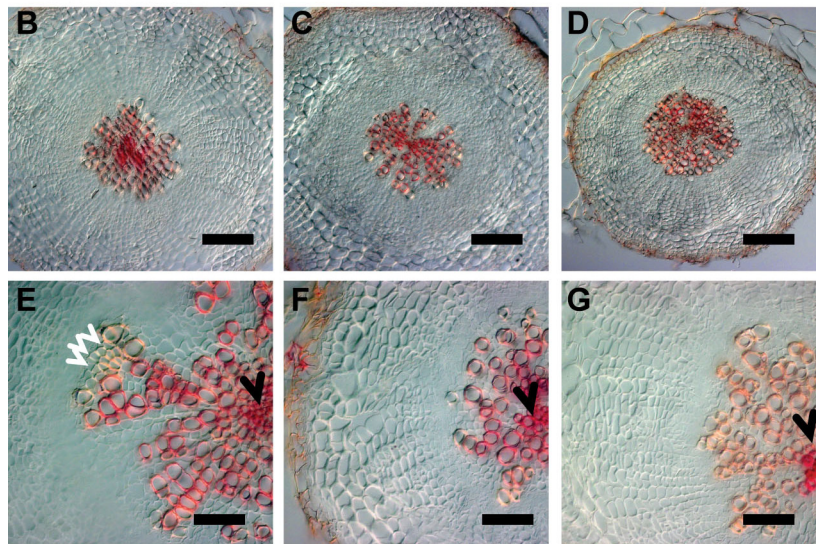
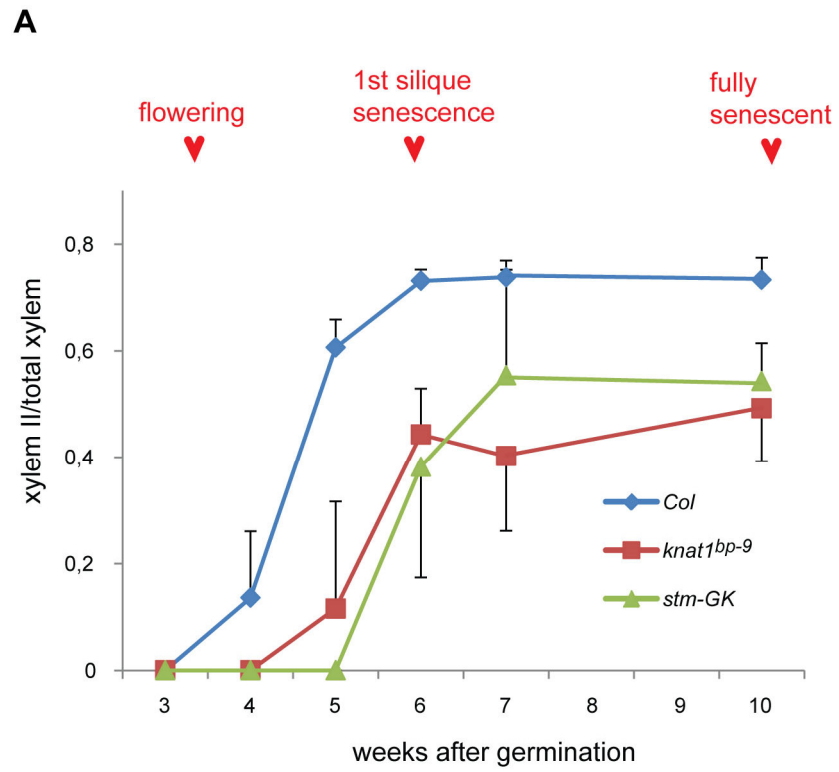


Fig. S7

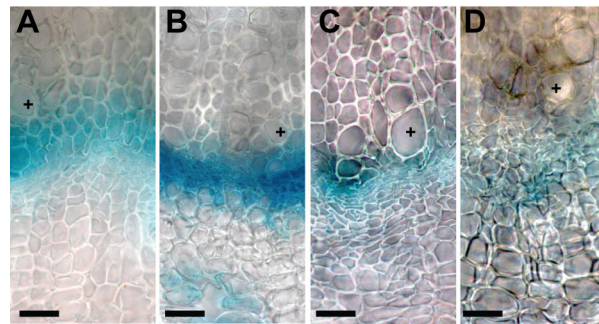


Fig. S8



Fig. S9

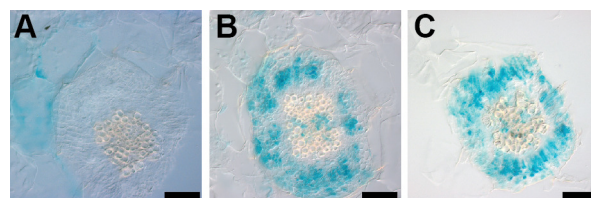


Fig. S10

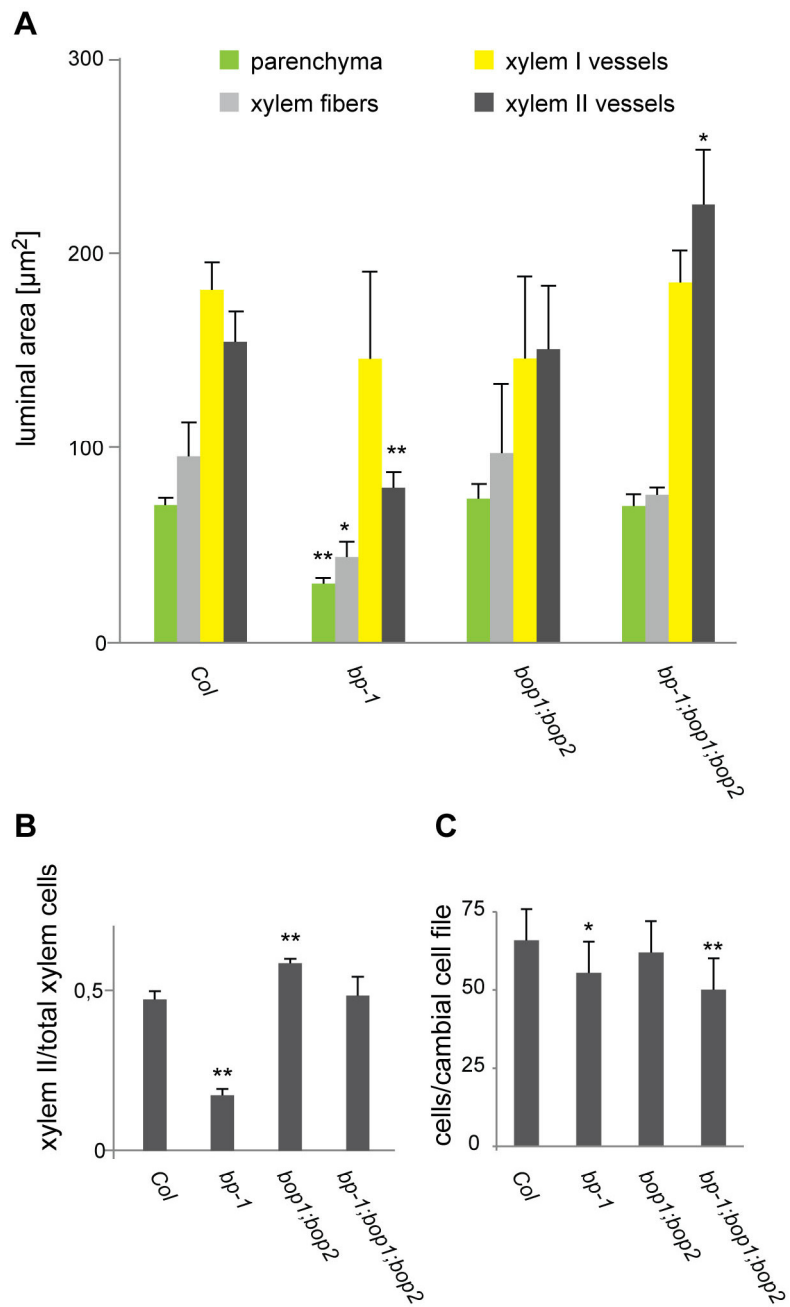


Table S1

Rank sum	AGI	alias	r-value (KNATI)	rank (KNATI)	r-value (STM)	rank (STM)	SCW regulon
5	At1g62360	<i>STM</i>	0.695	4	1.000	1	
7	At4g08150	<i>KNATI</i>	1.000	1	0.695	6	
9	At5g59310	<i>LTP4</i>	0.803	2	0.688	7	
16	At3g59845		0.678	7	0.681	9	
19	At2g28870		0.672	9	0.669	10	
21	At5g60910	<i>AGL8</i>	0.642	13	0.682	8	
24	At5g02030	<i>PNY</i>	0.607	21	0.805	3	
30	At2g31900	<i>XIF</i>	0.690	5	0.603	25	
30	At2g38090		0.626	16	0.656	14	
38	At4g21650		0.657	10	0.596	28	
43	At2g47160	<i>BORI</i>	0.601	24	0.624	19	
56	At1g11080	<i>SCPL31</i>	0.550	51	0.706	5	
56	At4g30520	<i>SARK</i>	0.571	35	0.614	21	
57	At3g59010	<i>PME35</i>	0.554	44	0.661	13	
64	At5g01200		0.576	32	0.589	32	
69	At4g29080	<i>IAA27</i>	0.629	15	0.556	54	
72	At2g29130	<i>LAC2</i>	0.558	41	0.589	31	Y
76	At5g44030	<i>CESA4/IRX5</i>	0.604	23	0.561	53	Y
79	At1g03170	<i>FAF2</i>	0.552	46	0.585	33	
79	At5g23810	<i>AAP7</i>	0.575	33	0.571	46	
80	At1g72230		0.717	3	0.536	77	Y
82	At5g03170	<i>FLA11</i>	0.592	25	0.553	57	Y
86	At1g12320	<i>DUF1442</i>	0.531	71	0.654	15	
88	At3g42950		0.542	61	0.600	27	Y
91	At5g60490	<i>FLA12</i>	0.626	17	0.541	74	Y
92	At2g42200	<i>SPL9</i>	0.550	49	0.574	43	
92	At4g27435	<i>DUF1218</i>	0.578	31	0.550	61	Y
93	At1g12430	<i>ARK3</i>	0.633	14	0.535	79	Y
96	At2g38080	<i>LAC4/IRX12</i>	0.581	28	0.546	68	
98	At4g13710		0.546	56	0.577	42	
100	At3g20100	<i>CYP705A19</i>	0.515	89	0.665	11	
103	At3g21190	<i>MSR1</i>	0.687	6	0.517	97	
103	At5g17420	<i>CESA7/IRX3</i>	0.539	63	0.580	40	Y
107	At1g60060		0.649	11	0.518	96	
108	At1g78490	<i>CYP708A3</i>	0.550	50	0.551	58	
111	At3g16920	<i>CTL2</i>	0.549	52	0.551	59	Y
112	At5g15630	<i>COBL4/IRX6</i>	0.552	47	0.548	65	Y
113	At2g37090	<i>IRX9</i>	0.522	83	0.591	30	Y
117	At3g18660	<i>GUX1</i>	0.546	55	0.549	62	Y
121	At4g23496	<i>SP1L5</i>	0.531	72	0.564	49	Y
121	At5g61480	<i>PXY</i>	0.507	97	0.607	24	
127	At5g25390	<i>SHN2</i>	0.568	37	0.522	90	
133	At4g18780	<i>CESA8/IRX1</i>	0.538	64	0.546	69	Y

Table S1, continued

Rank sum	AGI	alias	r-value (<i>KNAT1</i>)	rank (<i>KNAT1</i>)	r-value (<i>STM</i>)	rank (<i>STM</i>)	SCW regulon
134	At5g60020	<i>LAC17</i>	0.516	87	0.571	47	Y
139	At1g22480		0.528	76	0.548	63	
145	At1g80170		0.509	95	0.561	50	
148	At5g54690	<i>GAUT12/IRX8</i>	0.534	67	0.530	81	Y
149	At1g27440	<i>GUT2/IRX10</i>	0.530	74	0.540	75	Y
150	At1g47485	<i>CEP1</i>	0.537	65	0.524	85	
154	At2g33810	<i>SPL3</i>	0.506	98	0.555	56	
179	At3g50220	<i>IRX15</i>	0.513	90	0.522	89	Y
179	At3g62020	<i>GLP10</i>	0.525	80	0.516	99	Y

Table S1. Genes co-expressed with both *KNAT1* and *STM*. The 100 most strongly co-expressed genes for each *KNAT1* and *STM* were identified from a collection of more than 300 microarrays (Expression Angler; www.bar.utoronto.ca; Toufighi et al., 2004) and ranked in the order of decreasing r-values. Genes co-expressed with both *STM* and *KNAT1* are listed according to the sum of their rankings ($\text{rank}(\textit{KNAT1}) + \text{rank}(\textit{STM})$). Y, part of the SCW regulon according to Persson et al. (2005).

Table S2. Seed stocks.

line	mutagen/position	background	accession/donor	Reference
<i>knat1^{bp-9}</i>	dSpm, 1 st intron	<i>Col-0</i>	Dr. Angela Hay, Oxford University, UK	Dela Paz et al., 2012
<i>knat1^{bp-11}</i>	X-ray, deletion	<i>Col-1</i>	N3161	Dela Paz et al., 2012
<i>knat1^{bp-1}</i>	EMS, deletion	<i>Ler</i>	N30	Dela Paz et al., 2012
<i>knat1^{bp-1C}</i>	introgression of <i>knat1^{bp-1}</i>	<i>Col-0</i>		this work
<i>stm-GK</i>	T-DNA, 2nd intron	<i>Col-0</i>	N409575	this work
<i>stm-1</i>	EMS, nonsense mutation upstream of homeodomain	<i>Ler</i>	N8154	Long and Barton, 1998
<i>stm-1^C</i>	introgression of <i>stm-1</i>	<i>Col-0</i>		this work
<i>stm-4</i>	EMS	<i>Ler</i>	N12	Endrizzi et al., 1996
<i>stm-5</i>	EMS	<i>Ler</i>	N13	Endrizzi et al., 1996
<i>stm-6</i>	EMS	<i>Ler</i>	N14	Endrizzi et al., 1996
<i>knat2</i>	T-DNA, 3 rd intron	<i>Col-0</i>	N609159	this work
<i>knat3</i>	T-DNA, 1 st intron	<i>Col-0</i>	N636464	this work
<i>knat4</i>	T-DNA, 1 st intron	<i>Col-0</i>	N520216	this work
<i>knat5</i>	T-DNA, 1 st intron	<i>Col-0</i>	N616798	this work
<i>knat6</i>	T-DNA, 3 rd intron	<i>Col-0</i>	N617904	this work
<i>knat7</i>	T-DNA, 2 nd intron	<i>Col-0</i>	N610899	this work
<i>pKNAT1::GUS</i>		<i>Col-0</i>	N6141	Ori et al., 2000
<i>pSTM::GUS</i>		<i>Col-0</i>	Prof. Wolfgang Werr, University of Cologne, Germany	Kirch et al., 2003
<i>pATHB-8::GUS</i>		<i>Col-0</i>	N296	Baima et al., 1995
<i>Columbia-0 (Col-0)</i>	-	-	N28166	
<i>Landsberg erecta (Ler)</i>	-	-	N28445	
<i>bop1-5</i>	T-DNA, 1 st intron	<i>Col-0</i>	Sail14.c02	Norberg et al., 2005
<i>bop2-2</i>	T-DNA, 5'UTR	<i>Col-0</i>	N575879	Norberg et al., 2005
<i>pBOPI::GUS</i>		<i>Col-0</i>		Norberg et al., 2005
<i>pBOP2::GUS</i>		<i>Col-0</i>		Xu et al., 2010
<i>p35S::BOPI (bop1-6D)</i>	T-DNA, activation tagging	<i>Col-0</i>		Norberg et al., 2005

Table S3

Locus	Synonym	Primers	Use
AT3g18780	<i>ACT2</i>	TGGGATGAACCAGAAGGATG	expression
		AAGAATACCTCTCTTGGATTGTGC	expression
At1g62360	<i>STM</i>	CAAATGGCCTTACCCTTCG	expression
		GCCGTTTCCTCTGGTTTATG	expression
At4g08150	<i>KNAT1</i>	TCCCATTACATCCTCAACA	expression
		CCCCTCCGCTGTTATCTCT	expression
AT4G32410	<i>CesA1</i>	AAGAGCGACGAGCTATGAAGA	expression
		CCAGCCTTCTTCAGGGATTT	expression
AT4G39350	<i>CesA2</i>	TCATGCGCTAGAGAATGTCG	expression
		TGTTGCTTCAGATCTCTTCTCAAC	expression
AT5G05170	<i>CesA3</i>	CCAGATTGAGAGAGATTCAGAGAGT	expression
		AAACGTCGGAATAGTTCAAATCA	expression
AT5G44030	<i>CesA4</i>	CTGTGGTTATGAAGAGAAGACTGAA	expression
		TGCATTCTAAATCCAGTGAGGA	expression
AT5G09870	<i>CesA5</i>	TTACAAGCGCATCAAAGGAA	expression
		TCAAACCTCAAAATCAAGATCATCAA	expression
AT5G64740	<i>CesA6</i>	ACCCGGATTGATCACCATA	expression
		GAACCCAGAGACTCGTATCA	expression
AT5G17420	<i>CesA7</i>	TGACATGAATGGTGACGTAGC	expression
		CATCAAATGCTCCTTATCACCTT	expression
AT4G18780	<i>CesA8</i>	TTTGCTCTTGTGCTTACTGT	expression
		CAGCATGCTTGCTAGGTTTG	expression
AT2G21770	<i>CesA9</i>	GAAAATTCATCGTCCCTGAGA	expression
		CGTTACCGCAATGGACATAA	expression
AT2G25540	<i>CesA10</i>	TTGACCCACAACCTACCTGGTATC	expression
		TCTTTTGATGGGTCCAAGATTC	expression
AT3G57130	<i>BOP1</i>	GCTCGCGTTGCTTACTCAG	expression
		TGCTTCTTGAAGCTATGAGCA	expression
AT2G41370	<i>BOP2</i>	CGCCGTTGATCTTGCTCT	expression
		CCATGCTTGCCAATTGTTT	expression
AT4G32880	<i>ATHB8</i>	CTCAAGAGATTTACAACCTAACG	expression
		TCACTGCTTCGTTGAATCCTT	expression
AT1G32770	<i>SND1</i>	CAAGCTTGAGCCTTGGGATA	expression

Development 141: doi:10.1242/dev.111369: Supplementary Material

		TGGTCCCGGTTGGATACTT	expression
AT2G46770	<i>NST1</i>	GATGTCACCGTTCATGAGGTC	expression
		GGACTGTTTAGGGTTTTGTGAAG	expression
AT4G28500	<i>SND2</i>	CCCTTCTTGTGGCCATAACTT	expression
		GCCTTCAAGATGCTCCAAGA	expression
AT1G71930	<i>VND7</i>	CACGAATACCGTCTCCAAAACCT	expression
		CCTAAATGCTCGACACACCA	expression
AT1G46480	<i>WOX4</i>	CATCATCGTCACTAGACATTATGAGA	expression
		CCTCTTGTACTCATTCTCTTCCACT	expression
AT1G79430	<i>APL</i>	TGGATATTCAGCGCAACGTA	expression
		TGCACTTCCATTTGCATCTC	expression
AT5G61480	<i>TDR</i>	TTCAAACCGACGAATCCATGT	expression
		TTATCCACTTGTAAGTGTAAGCATATTCT	expression
AT1G70510	<i>knat2</i>	GAGTTTGTCTTGCCTTCATG	genotyping
		TCCAGCTAGTTCTTATCAGGTGG	genotyping
AT5G25220	<i>knat3</i>	TCTCCTTCAATCATTTCACCG	genotyping
		ACATCTAATCCCCATCGAAC	genotyping
AT5G11060	<i>knat4</i>	AACTTTAGAAGCCGCTCAAGG	genotyping
		TGACAAGTTCTTGGTTGATTGG	genotyping
AT4G32040	<i>knat5</i>	TTCGGAGATGCAAAATACTGG	genotyping
		TTGATGTACCATTGGAGCTTG	genotyping
AT1G23380	<i>knat6</i>	TTATCCCTCTCTGGTTCGGTC	genotyping
		GCAGATAAGAGTGCCCACTTG	genotyping
AT1G62990	<i>knat7</i>	TTGCCACCAATT TTTCAAGAC	genotyping
		TGCCGTGAAATTGAGAACAAC	genotyping
At1g62360	<i>stm-1</i>	AAGTCGATATGAACAATGAATTTGTAGATGCA	
		GACGGCTCCACCAATCAAGCA	
AT3G57130	<i>bop1-5</i>	GTCGATCTCTCTTTAGATATTTTAG	genotyping
		GAATTCATAACCAATCTCGATACAC	
AT2G41370	<i>bop2-2</i>	CCGGTTCATCCATTCAAATCTCT	genotyping
		TGGTTCACGTAGTGGGCCATCG	
AT3G57130	<i>BOP1</i>	GTCGATCTCTCTTTAGATATTTTAG	genotyping
		TTTACGCGACTATGGTTCAAGAG	
AT2G41370	<i>BOP2</i>	CCGGTTCATCCATTCAAATCTCT	genotyping
		TTGTTGGGCTAGCGGGTACG	

Supplementary references

Ori N, Eshed Y, Chuck G, Bowman JL, Hake S (2000) Mechanisms that control knox gene expression in the Arabidopsis shoot. *Development* 127: 5523-5532.

Kirch T, Simon R, Grunewald M, Werr W (2003) The DORNROSCHEN/ENHANCER OF SHOOT REGENERATION1 gene of Arabidopsis acts in the control of meristem cell fate and lateral organ development. *Plant Cell* 15: 694-705.